CrystEngComm

Accepted Manuscript

ROYAL SOCIETY OF CHEMISTRY

www.rsc.org/crystengcomm

CrystEngComm RSCPublishing

ARTICLE

Cite this: DOI: 10.1039/x0xx00000x

Received 00th January 2015,
Accepted 00th January 2015

DOI: 10.1039/x0xx00000x

www.rsc.org/

Crystal engineering of cadmium coordination polymers decorated by nitro-functionalized thiophene-2,5-dicarboxylate and structurally related bis(imidazole) ligands with varying flexibility

Li-Ping Xue,[a] Zhao-Hao Li,[a] Lu-Fang Ma,*[a] and Li-Ya Wang*[a,b]

A new thiophene-2,5-dicarboxylic acid derivative, 3-nitro-thiophene-2,5-dicarboxylic acid (H_2ntdc), was synthesized. Reaction of H_2ntdc with cadmium diacetate dihydrate and structurally related bis(imidazole) ligands with varying flexibility gave rise to four new CPs, formulated as $\{[Cd(ntdc)(bmip)(H_2O)](H_2O)\}_n$ (**1**), $\{[Cd(ntdc)(bmib)](H_2O)\}_n$ (**2**), $[Cd(ntdc)(beip)]_n$ (**3**) and $[Cd(ntdc)(beib)]_n$ (**4**) [bmip = 1,3-bis(2-methylimidazolyl)propane, bmib = 1,4-bis(2-methylimidazolyl)butane, beip = 1,3-bis(2-ethylimidazolyl)propane and beib = 1,4-bis(2-ethylimidazolyl)butane]. Moreover, a new compound $\{[Cd(ntc)_2(bmib)](H_2O)\}_n$ (**5**) (Hntc = 4-nitro-thiophene-2-carboxylic acid) involving *in situ* ligand synthesis was prepared. Structural analyses reveal that **1** features a two-dimensional (2D) 4^4-**sql** layer, and is further stacked *via* hydrogen bonding interactions to give a three-dimensional (3D) hydrogen-bonded architecture. **2** displays a 3,4-connected 3D network with **ins** type topology, which is composed of 2D **hcb** topological networks pillared by bmib ligands. **3** exhibits a 3,5-connected 3D network with $(4^2.6^3.8^5)(4^2.6)$ topology. **4** possesses a 3-fold interpenetrating 3D net with **dmp** topology. **5** can be described as a a one-dimensional (1D) chain structure, and is further assembled into a 2D hydrogen-bonded 4^4 **sql** layer. Factors that influence the structural assembly of **1**−**4**, as well as the formation of **5** involving *in situ* produced Hntc ligand are discussed. Moreover, structure stabilities and photoluminescent properties of the complexes were also investigated.

Introduction

Owing to aesthetic appeal of fascinating structural topologies and potential applications as functional materials, research on coordination polymers (CPs) are currently of considerable interest.[1] Despite tremendous progress, the synthesis of CPs with predictable structures and specific properties is still a great challenge because some intrinsic and external factors have important influence on the crystallization process.[2] In this regard, the choice of suitably-tailored organic ligands is undoubtedly the key to control and adjust the architectures of CPs. So far, multidentate aromatic dicarboxylate ligands have proven to be the most popular linkers in the construction of CPs, as they possess structural rigidity, chemical robustness and versatile binding modes. Some earlier reports relate to the use of benzene-, pyridine-, imidazole-, and thiophene-based dicarboxylates linkers that are inter-bridged by mono- or multi-nuclear metal nodes, leading to stable CPs with expectant topologies.[3] Moreover, as known, the electronic and steric effects of aromatic substituent groups have a significant impact on coordination-driven self-assembly.[4] However, in contrast to commercially available benzenedicarboxylates with substituted R (OH, NO_2, Me, CF_3, OCH_3) groups which have been extensively explored, there are only limited known examples of CPs with substituted heterocyclic dicarboxylates.[5]

Thiophene-2,5-dicarboxylic acid (H_2tdc) with C2-like symmetry, as a good exo-bidentate bridging ligand, has been to bulid CPs with diversified topologies and interesting properties.[6] Our current interest is to incorporate sterically hindered groups into the H_2tdc backbone, and expect the employment of H_2tdc derivatives can not only create robust CPs, but can also endow structure-driven properties. Moreover, as well known, the flexible bis(imidazole) ligands with excellent coordinating ability and variable conformations have been widely used to regulate the structures of CPs with aromatic dicarboxylate ligands by varying the ligands' steric

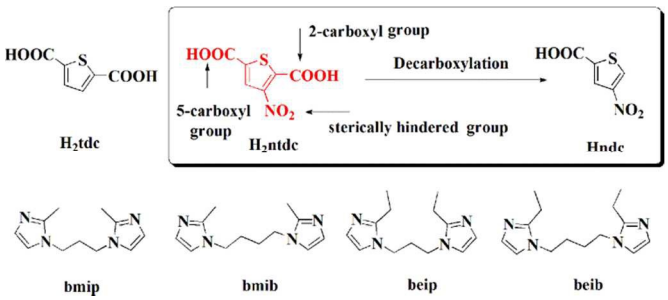

Scheme 1 Ligands relevant to this work. Ligands in rounded rectangle are synthetically or *in situ* synthetically used.

hindrance and lengths.

Inspired by the above considerations, in this work, four cadmium CPs, $\{[Cd(ntdc)(bmip)(H_2O)](H_2O)\}_n$ (**1**), $\{[Cd(ntdc)(bmib)](H_2O)\}_n$ (**2**), $[Cd(ntdc)(beip)]_n$ (**3**), and $[Cd(ntdc)(beib)]_n$ (**4**) were synthesized from the reactions of cadmium diacetate dihydrate with a newly synthesized 3-nitro-thiophene-2,5-dicarboxylic acid (H_2ntdc) in the presence of structurally related bis(imidazole) ligands with different steric hindrance and lengths (Scheme 1). Furthermore, a new compound $\{[Cd(ntc)_2(bmib)](H_2O)\}_n$ (**5**) (Hntc = 4-nitro-thiophene-2-carboxylic acid) involving *in situ* decarboxylation of H_2ntdc has been obtained at higher reaction temperature. The results indicate H_2ntdc is an effective building block in constructing CPs with diverse architectures at relatively lower reaction temperature. Moreover, structure stabilities and photoluminescent properties of the complexes were also investigated.

Experimental section

Materials and general techniques

All reagents and solvents employed were reagent grade quality, obtained commercially and used without further purification. Bis(imidazole) ligands bmip, bmib, beip and beib were synthesized according to the literatures.[7] The IR spectra were recorded as KBr pellets on a Nicolet Avatar-360 spectrometer in the range of 4000 to 400 cm^{-1}. ^1H NMR spectra was measured with a Bruker AVANCE-400 NMR spectrometer. Elemental analyses for C, H, and N were carried out on a Flash 2000 elemental analyzer. Powder X-ray diffraction (PXRD) measurements were performed on a Bruker D8-ADVANCE X-ray diffractometer with Cu Kα radiation (λ =1.5418 Å). Thermogravimetric analyses (TGA) were carried out on a SDTQ600 thermogravimetric analyzer. A platinum pan was used for heating the sample with a heating rate of 10 °C/min under a N_2 atmosphere. Fluorescence measurements were recorded with a Hitachi F4500 fluorescence spectrophotometer.

Synthesis of H_2ntdc

A solution of dimethyl thiophene-2,5-dicarboxylate (10.0 g, 50 mmol) in concentrated sulphuric acid (60 mL) at 0 °C was added slowly concentrated HNO_3 (3.4 mL) and the resulted solution was further stirred for about 3 h at 0 °C. Then the mixture was added to 500 ml ice-water, the resulted white solid was collected *via* vacuum filtration, washed with 1000 mL ice water and dried in air. Yield 11.5 g (92%). The second step was to dissolve the isolated dimethyl-3-nitro-thiophene-2,5-dicarboxylate (2.54 g, 10 mmol) in 20% HCl aqueous solution (40 mL). The mixture was refluxed for 6 h, resulting in a clear solution. After cooled down to room temperature, the solvent was removed to yield a gray hydrophilic powder. Yield: 1.96 g (90%). IR (cm^{-1}): 3391 (br), 3049 (w), 2871 (w), 1682 (s), 1529 (s), 1488 (w), 1399 (w), 1377 (m), 1327 (m), 1234 (s), 883 (m), 793 (m), 746 (m), 727 (m); ^1H-NMR (D_2O): 7.85 (1H, s). Elemental analysis calcd (%) for $C_6H_3NO_6S$: C, 33.18; H, 1.38; N, 6.45. Found: C, 33.16; H, 1.40; N, 6.43.

Synthesis of Hntc

Hntc was synthesized following experimental procedure: H_2ntdc (0.22 g, 10 mmol) was added to a 100 mL Pyrex glass tube containing 25 mL of neat water and the mixture was heated at 120 °C for 3 h under autogenous pressure. Afterwards, the tube was cooled to room temperature slowly. The subsequent removal of water under reduced pressure produced Hntc as an off-white solid in quantitative yield. IR (cm^{-1}): 3037 (w), 1679 (s), 1525 (s), 1479 (w), 1397 (w), 1375 (m), 1323 (m), 1235 (s), 883 (m), 797 (m), 735 (m), 726 (m); ^1H-NMR (D_2O): 8.63 (1H, s), 8.07 (1H, s). Elemental analysis calcd (%) for $C_5H_3NO_4S$: C, 34.68; H, 1.73; N, 8.09. Found: C, 34.59; H, 1.78; N, 8.13.

Synthesis of $\{[Cd(ntdc)(bmip)(H_2O)](H_2O)\}_n$ (1)

A mixture of H_2ntdc (21.7 mg, 0.1 mmol), $Cd(OAc)_2{\cdot}2H_2O$ (26.7 mg, 0.1 mmol), bmip (20.4 mg, 0.1 mmol), NaOH (4.00 mg, 0.10 mmol), and 7 mL deionized water was sealed in a 20 mL Pyrex glass tube and heated at 60 ºC for 72 h, followed by cooling to room temperature at a rate of 5 $^oC\ h^{-1}$. Yellow crystals were collected (yield: 49% based on Cd). Elemental analysis calcd (%) for $C_{17}H_{21}N_5O_8SCd$: C, 35.93; H, 3.70; N, 12.33. Found: C, 35.89; H, 3.72; N, 12.30. IR (cm^{-1}): 3305 (m), 3131 (w), 2943 (w), 1658 (m), 1578 (s), 1519 (m), 1479 (w), 1401 (m), 1352 (vs), 1315 (m), 1298 (w), 1282 (w), 1150 (s), 1095 (w), 1080 (w), 999 (m), 943 (w), 868 (m), 820 (s), 790 (w), 747 (s), 693 (w), 681 (m).

Synthesis of $\{[Cd(ntdc)(bmib)](H_2O)\}_n$ (2)

The synthesis of **2** was similar to that of **1**, but with bmib (21.8 mg, 0.1 mmol) in place of bmip. Yellow crystals were obtained (yield: 53% based on Cd). Elemental analysis calcd (%) for $C_{18}H_{21}N_5O_7SCd$: C, 38.30; H, 3.72; N, 12.41. Found: C, 38.27; H, 3.77; N, 12.45. IR (cm^{-1}): 3505 (m), 3484 (m), 3118 (w), 2948 (w), 1645 (m), 1596 (s), 1559 (s), 1540 (m), 1516 (m), 1478 (w), 1453 (w), 1400 (s), 1349 (s), 1339 (s), 1314 (m), 1294 (w), 1278 (w), 1179 (w), 1151 (s), 1128 (w), 1100 (w), 1073 (w), 1005 (w), 966 (w), 939 (m), 868 (m), 819 (s), 778 (m), 756 (m), 683 (w), 680 (m).

Synthesis of $[Cd(ntdc)(beip)]_n$ (3)

The synthesis of **3** was similar to that of **1**, but with beip (23.2 mg, 0.1 mmol) in place of bmip. Colorless crystals were obtained (yield: 53% based on Cd). Elemental analysis calcd

Table 1 Crystal data and structure refinements for **1–5**

Compounds	**1**	**2**	**3**	**4**	**5**
Formula	$C_{17}H_{21}N_5O_8SCd$	$C_{18}H_{21}N_5O_7SCd$	$C_{19}H_{21}N_5O_6SCd$	$C_{20}H_{22}N_6O_8SCd$	$C_{22}H_{24}N_6O_9S_2Cd$
M_r	567.85	563.86	559.87	618.90	692.99
Crystal system	Monoclinic	Monoclinic	Monoclinic	Orthorhombic	Monoclinic
Space group	*P*2(1)/*c*	*P*2(1)/*c*	*C*2/*c*	*Pnna*	*P*2(1)/*c*
a (Å)	10.331(2)	6.941(2)	12.7557(5)	9.4744(4)	8.9864(4)
b (Å)	13.446(3)	24.440(8)	15.4715(5)	17.5789(8)	15.9532(8)
c (Å)	16.188(3)	13.040(4)	22.2958(8)	14.4100(7)	20.1727(10)
β (°)	110.858(9)	107.867(13)	96.9060(10)	90	101.4630(10)
V (Å^3)	2164.3(7)	2105.4(11)	4368.1(3)	2399.98(19)	2834.3(2)
Z	4	4	8	4	4
ρ(g cm^{-3})	1.743	1.779	1.703	1.713	1.624
μ (mm^{-1})	1.160	1.189	1.142	1.056	0.977
F(000)	1144	1136	2256	1248	1400
GOF(F^2)	1.070	1.024	1.062	1.082	1.046
$R_1{}^a$ [$I>2\sigma(I)$]	0.0507	0.0871	0.0298	0.0381	0.0267
$wR_2{}^b$[$I>2\sigma(I)$]	0.1252	0.1871	0.0634	0.1048	0.0656

^{a} $R_1 = \sum\left||F_o|-|F_c|\right| / \sum|F_o|$. ^{b} $wR_2 = \{\sum[w(F_o^2-F_c^2)^2] / \sum[w(F_o^2)^2]\}^{1/2}$

(%) for $C_{19}H_{21}N_5O_6SCd$: C, 40.72; H, 3.75; N, 12.50. Found: C,40.69; H, 3.79; N, 12.48. IR (cm^{-1}): 3105 (w), 2946 (w), 1646 (m), 1589 (s), 1556 (s), 1543 (m), 1518 (m), 1459 (w), 1401 (s), 1337 (s), 1332 (s), 1315 (m), 1290 (w), 1276 (w), 1177 (w), 1153 (s), 1126 (w), 1109 (w), 1005 (w), 967 (w), 940(m), 869 (m), 823 (s), 778 (m), 758 (m), 687 (w), 668 (m).

Synthesis of [Cd(ntdc)(beib)]$_n$ (4)

The synthesis of **4** was similar to that of **1**, but with beib (24.6 mg, 0.1 mmol) in place of bmip. Yellow crystals were obtained (yield: 61% based on Cd). Elemental analysis calcd (%) for $C_{20}H_{22}N_6O_8SCd$: C, 38.78; H, 3.56; N, 13.57. Found: C, 38.67; H, 3.67; N, 13.55. IR (cm^{-1}): 3107 (w), 2942 (w), 1644 (m), 1593 (s), 1557 (s), 1540 (m), 1516 (m), 1478 (w), 1453 (w), 1400 (s), 1349 (s), 1339 (s), 1314 (m), 1294 (w), 1278 (w), 1179 (w), 1152 (s), 1124 (w), 1100 (w), 1079 (w), 1005 (w), 968 (w), 941 (m), 867 (m), 819 (s), 778 (m), 756 (m), 683 (w), 680 (m).

Synthesis of {[Cd(ntc)$_2$(bmib)](H$_2$O)}$_n$ (5)

The synthesis of **5** was similar to that of **2**, using the same components in the same molar ratio except that the reaction temperature was fixed at 120 ºC. Yellow crystals of **5** were obtained (yield: 36% based on Cd). **5** was also synthesized following the procedure. A mixture of Hntc (34.6 mg, 0.2 mmol), Cd(OAc)$_2$·2H$_2$O (26.7 mg, 0.1 mmol) and bmib (21.8 mg, 0.1 mmol) was dissolved in 7 mL deionized water. The final mixture was placed in a 20 mL Pyrex glass tube under autogenous pressure and heated at 120 °C for 3d, followed by cooling to room temperature at a rate of 5 °C h^{-1}. Crystals of **5** were collected in 56 % yield. Elemental analysis calcd (%) for $C_{22}H_{24}N_6O_9S_2Cd$: C, 38.10; H, 3.46; N, 12.12. Found: C, 38.12; H, 3.50; N, 12.10. IR (cm^{-1}): 3419 (m), 3115 (w), 2971 (w), 1646 (m), 1569 (m), 1517 (s), 1402 (m), 1363 (s), 1336 (w), 1278 (w), 1152 (m), 1100 (w), 1057 (m), 998 (m), 880 (m), 811 (m), 733 (w), 686 (m), 669 (w).

X-ray crystallography

The crystal structure data of **1**−**5** were collected on Bruker SMART APEX II CCD diffractometer equipped with a graphite-monochromated Mo Kα (λ= 0.71073 Å) radiation using an ω scan mode at 293 K. An empirical absorption correction was applied using the SADABS program.[8] The structures were solved by direct methods and refined by full-matrix least-squares on F^2 using the SHELXL-97 program package.[9] All non-hydrogen atoms were refined anisotropically. The hydrogen atoms on water molecules were located from difference Fourier maps and were refined using riding model. Other hydrogen atoms were placed at the calculation positions. The disordered C atoms in **3** (C17) and the disordered C, N and O atoms in **4** (C6, C7, N3, O3, O4) were refined using C, N and O atoms split over two sites, with a total occupancy of 1. A summary of the crystallographic data, selected bond lengths and hydrogen bond parameters are listed in in Table 1, Table S1 and Table S2 of ESI, respectively. Topology information for **1**–**5** were obtained using TOPOS4.0 program package.

Results and discussions

Synthesis of compounds 1–5

According to our experimental results, the reaction variables, such as metal-ligand ratio, temperature, and pH value play important roles in the construction of **1**–**5.** In each synthetic case, an approximately equimolar amount of reagents was used for the starting materials. Furthermore, the temperature is crucial and parallel experiments with different temperatures showed that **1**–**4** were obtained at 60 ºC while **5** at 120 ºC. Significantly, the amount of sodium hydroxide is a key point

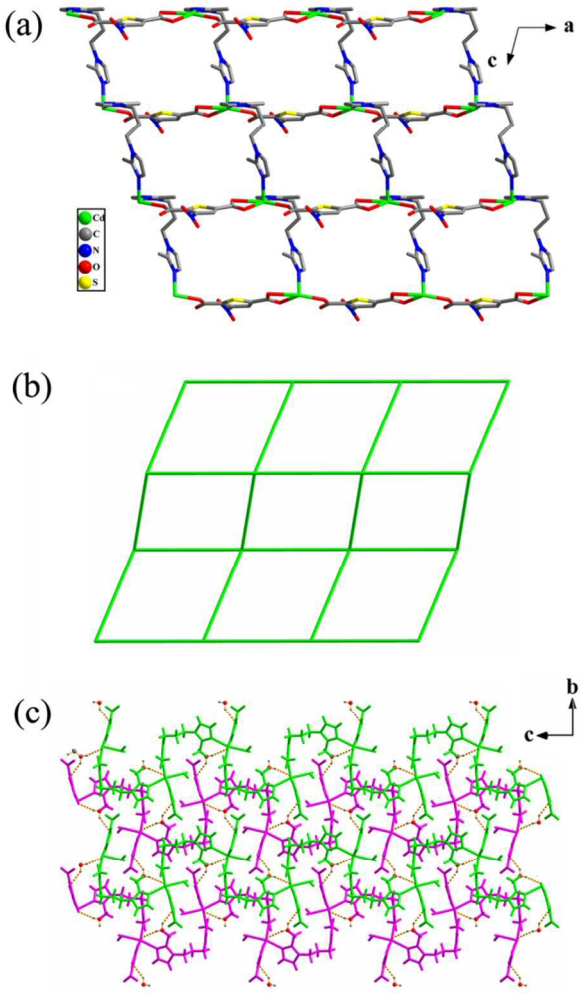

Fig. 1 (a) View of the 2D layer structure in **1**. (b) 2D pleated sheet with (4,4) **sql** topology. (c) View of 3D hydrogen-bonded network formed through hydrogen-bonding interactions. The hydrogen atoms are omitted for clarity.

for the fabrication of the resulting CPs, and when the amount was changed, only clear yellow solution or uncharacterized precipitate were obtained. Various coordination modes of H_2ntdc ligand observed in compounds **1**–**4** are shown in Scheme 2, and the further structural details are described below. In addition, compounds **1**–**5** were stable towards oxygen and moisture, and almost insoluble in common organic solvents. In the IR spectra of **1**–**5**, there are no absorption bands in the range 1710–1675 cm^{-1}, which proves the complete deprotonation of all the carboxyl groups. The characteristic bands of the deprotonated carboxylate groups appear in the region 1658–1569 cm^{-1} for the antisymmetric stretching and 1352–1314 cm^{-1} for the symmetric ones. Moreover, there appears a broad band at about 3300 for **1**, 3505 for **2** and 3419 cm^{-1} for **5**, which corresponds to water molecules, respectively.

Crystal Structure of $\{[Cd(ntdc)(bmip)(H_2O)](H_2O)\}_n$ (1)

Complex **1** crystallizes in a monoclinic space group $P2_1/c$ and the asymmetric unit is composed of one Cd^{2+} ion, one $ntdc^{2-}$ anion, one bmip ligand, one coordinated water molecule and one lattice water molecule in the lattice (Fig. S1†). The Cd^{2+} ion shows a distorted octahedral geometry, coordinated by three oxygen atoms from two $ntdc^{2-}$ anions, two nitrogen atoms from a pair of bimp ligands and one oxygen atom from one guest water molecule. The Cd1–O4 distance (2.604 Å) is significantly longer than the other Cd–O distances (2.226–2.389Å), reflecting the dissymmetric coordination of the carboxylate groups. In the present case, each $ntdc^{2-}$ anion in a bidentate μ_2-(η^1,η^1)-(η^1) bridging mode (Mode I, Scheme 2) links two Cd^{2+} ions, resulting in a 1D chain along *a* axis. The dihedral angle between two coordinated carboxylates is 5.983°. The Cd^{2+} ions in the 1D chains are further connected by bmip ligands assuming the *anti-gauche* conformation, forming a 2D pleated sheet with 4^4-**sql** topology along the crystallographic *ac* plane (Fig. 1a and Fig. 1b). The 2D bilayers are further linked together *via* intermolecular hydrogen bonds between water molecules and carboxylate oxygen atoms to generate a 3D hydrogen-bonded network (Fig. 1c). Moreover, this structure also contains interlayer π–π stacking between the parallel thiophene ring and/or 2-methyl imidazole ring of bmip in an offset fashion with the centroid-centroid distance of 3.675 Å and 3.780 Å, as well as interlayer C−H···π interactions with an edge-to-face orientation (*d* =2.97 Å, *A* =129°, *d* and *A* stand for H···π separations and C−H···π angles in the C−H···π patterns, respectively), which further promote the stability and integrity of the 3D supramolecular network.

Crystal Structure of $\{[Cd(ntdc)(bmib)](H_2O)\}_n$ (2)

As compared to complex **1**, the bmip coligand is replaced by bmib, and the resulting structure is a (3,4)-connected 3D **ins** network. Complex **2** crystallizes in $P2_1/c$ space group and its asymmetric unit consists of one Cd^{2+} ion, one $ntdc^{2-}$ anion, one bmib and one lattice water molecule (Fig. S2†). Each distorted octahedral Cd^{2+} ion is defined by four carboxylate oxygen atoms from three $ntdc^{2-}$ anions and two nitrogen atoms from two bmib ligands. The bond lengths of Cd–N are 2.246 (Cd–N1) and 2.221 Å (Cd–N4), while the Cd–O bond lengths range from 2.323 to 2.481 Å, which are in the normal range. All $ntdc^{2-}$ anions take the μ_3-(η^1,η^1)-(η^1,η^1) coordination mode (Mode II, Scheme 2), in which two carboxylate groups attain different orientations with a 87.724° dihedral angle. The carboxylate group at the 2-position adopts the *anti–anti* η^1:η^1 bridging mode linking Cd^{2+} ions to generate 1D chains with Cd···Cd distance of 6.9410 Å, which are linked *via* the η^1:η^1 chelating fashion of carboxylate group at the 5-position to form 3-connected 2D **hcb** shubnikov hexagonal plane layer along the *ac* plane (Fig. 2a and Fig. 2b). Such layers are further bridged by bmib with the *anti-anti-gauche* mode, resulting in a 3D structure (Fig. 2c). As such, topologically, Cd^{2+} ions and $ntdc^{2-}$ anions act as 3-connected and 4-connected nodes, respectively, giving rise to a dinodal (3,4)-connected 3D **ins** network with the Schläfli symbol of $(6^3)(6^5.8)$ (Fig. 2d).

Intermolecular hydrogen bonding interactions [O···O distances: O(7)···O(4) =3.016 Å, O(7)···O(3) =2.997 Å, O(7)···S(1) =3.351 Å; and O–H···O angels: O(7)–H(1W)···O(4)

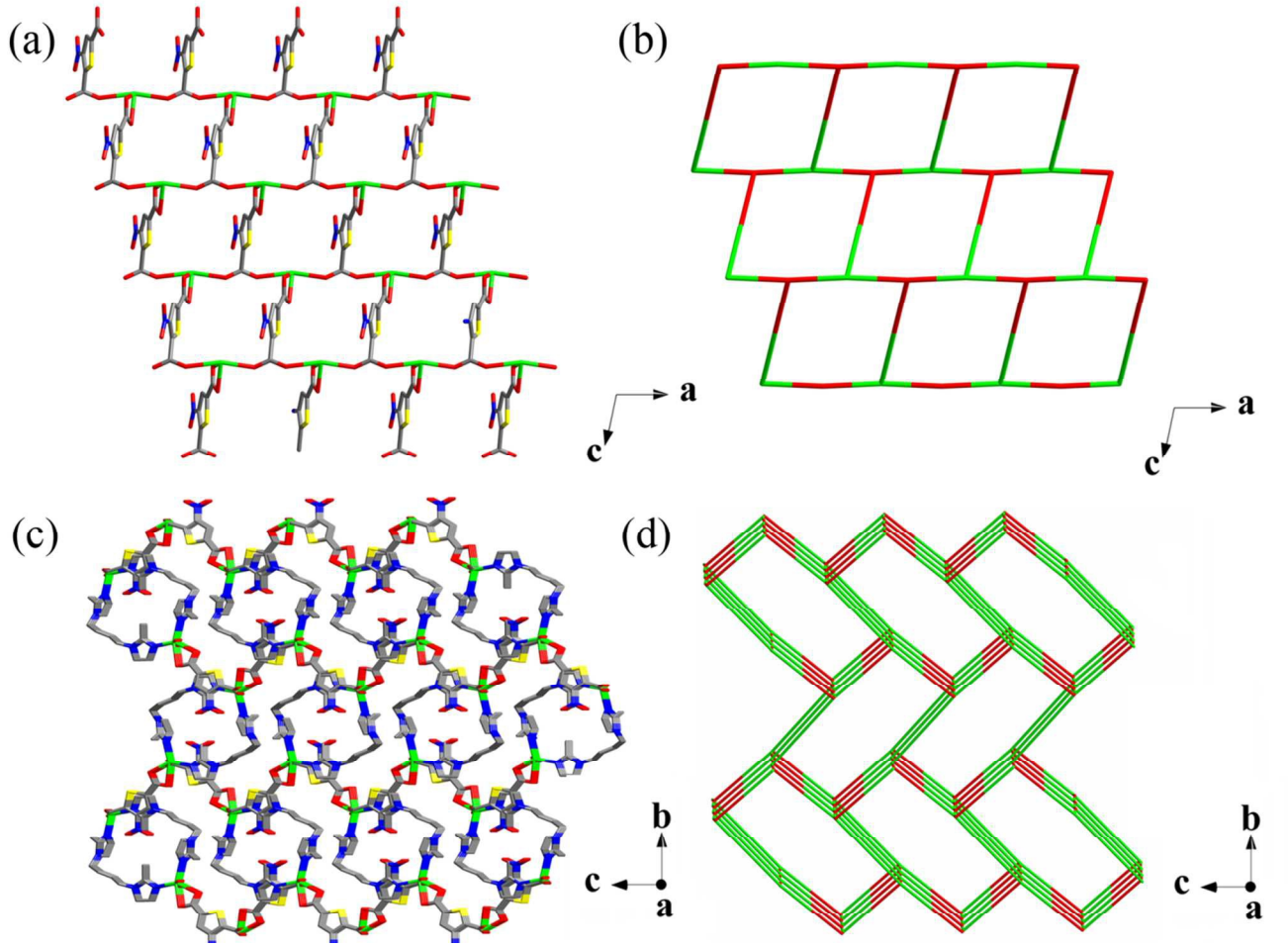

Fig. 2 (a) View of the 2D layer structure constructed by Cd^{2+} ions and $ntdc^{2-}$ anions in **2**. (b) 3-connected 2D **hcb** net. (c) A perspective of 3D framework along the *bc* plane. (d) Schematic representation of the 3D (3,4)-connected **ins** network of **2**. The hydrogen atoms are omitted for clarity.

=179.29°, O(7)–H(2W)···O(3) =179.38°, O(7)–H(1W)···S(1) =111.28°] between lattice water molecule and carboxylate oxygen atoms or thiophene sulfur atoms are also observed to stabilize this structure. Furthermore, π–π stacking interactions are found between the thiophene rings and the 2-methyl imidazole rings with the centroid–centroid separations of 3.478–3.548 Å, as well as C–H···π interactions with an edge-to-face orientation (d =2.94 Å; A =122° in the C–H···π patterns).

Crystal Structure of $[Cd(ntdc)(beip)]_n$ (3)

Complex **3** shows a 3D framework structure. There are one Cd^{2+} ion, one $ntdc^{2-}$ anion and one beip ligand in the asymmetric unit (Fig. S3†). Cd^{2+} ion is six-coordinated by four oxygen atoms from three different $ntdc^{2-}$ anions and two nitrogen atoms from two beip ligands in a distorted octahedral coordination environment. The Cd–O and Cd–N bond distances fall in the range of 2.249–2.404 and 2.269–2.332 Å, respectively. In **3**, each $ntdc^{2-}$ anion also exhibits the tridentate μ_3-(η^1,η^1)-(η^1,η^1) coordination fashion to connect three adjacent Cd^{2+} ions, but unlike that of **2**, Cd^{2+} ions are bridged by the bridging $ntdc^{2-}$ anion to yield a double chain structure (Fig. 3a). The extension of the structure into a 3D network is accomplished by interlinking these 1D chains through beip ligands, which assume the *anti-gauche* conformation (Fig. 3b). In topology, the structure could be simplified to be a 3,5-connected net with a point symbol of $(4^2.6^3.8^5)(4^2.6)$ by denoting $ntdc^{2-}$ anions as 3-connected nodes and Cd^{2+} ions as 5-connected linkers (Fig. 3c).

Crystal Structure of $[Cd(ntdc)(beib)]_n$ (4)

Complex **4** crystallizes in the orthorhombic *Pnna* space group, revealing a 3-fold interpenetrating 3D net with **dmp** topology. The asymmetric unit contains a half crystallographically independent Cd^{2+} ion, a half $ntdc^{2-}$ anion and a half beib moiety. As shown in Fig. S4, the Cd^{2+} ion, lying in a binary axis, is coordinated by four carboxylate oxygen atoms from two $ntdc^{2-}$ anions and two nitrogen atoms of two beib ligands to furnish a distorted trigonal prismatic coordination geometry. The bond lengths of Cd–O are 2.265 (Cd–O1) and 2.514 Å (Cd–O2), while Cd–N bond length is 2.237(4) Å. In **4**, each $ntdc^{2-}$ anion serves as a bridge linking two adjacent Cd^{2+} ions by adopting the μ_2-(η^1,η^1)-(η^1,η^1) coordination mode (Mode III, Scheme 2), to generate a 1D zigzag chain along *b* axis (Fig. 4a). As a

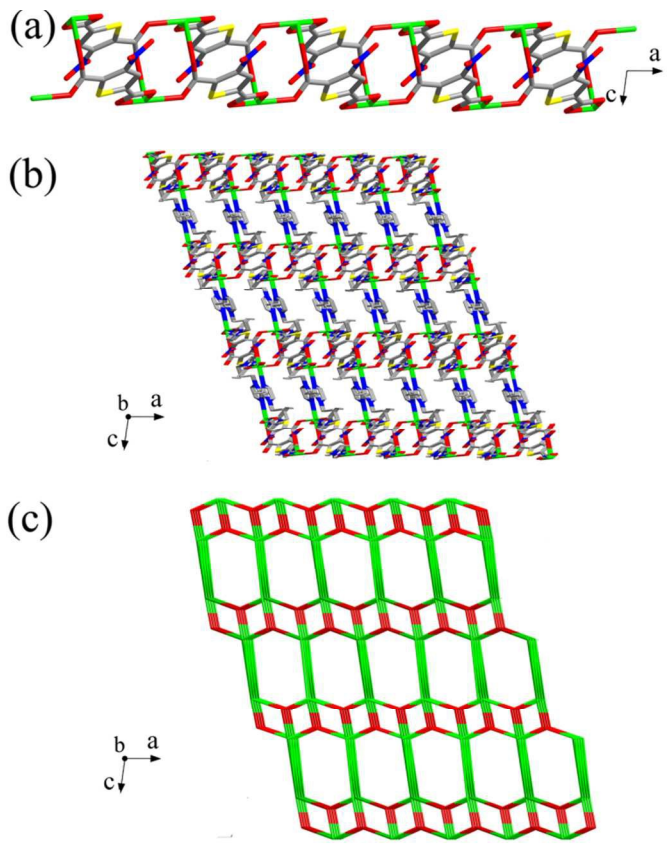

Fig. 3 (a) View of the double chain structure in **3**. (b) A perspective of 3D framework through beip ligands. (c) Schematic representation of the 3D (3,5)-connected network of **3**. The hydrogen atoms are omitted for clarity.

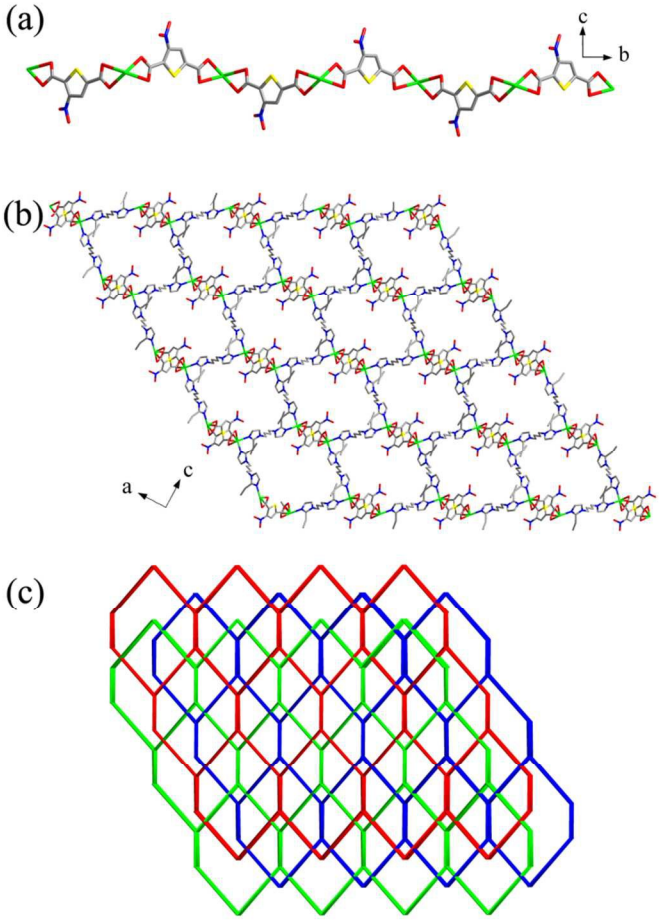

Fig. 4 (a) View of the zigzag chain in **4**. (b) A single 3D framework of **4**. (c) Schematic view of the 3-fold interpenetration based on 4-connected 3D **dmp** topology. The hydrogen atoms are omitted for clarity.

consequence, the 1D chains are further extended by the beib spacers assuming the *anti-anti-anti* conformation to afford a 3D coordination network (Fig. 4b). Topologically, both μ_2-ntdc^{2-} anions and beib ligands serve as the linear connectors, and each Cd^{2+} ion is 4-connected. Thus, the overall 3D network shows a uniform 4-connected **dmp** net with (6^5.8) topology. Owing to the spacious nature of the single network, it allows three independent equivalent networks to interpenetrate in a normal mode, resulting in a 3-fold interpenetrating network (Fig. 4c).

Crystal Structure of {[Cd(ntc)$_2$(bmib)](H$_2$O)}$_n$ (5)

Under similar synthesis condition of **2**, except for the reaction temperature, a 2D supramolecular structure is constructed. Complex **5** crystallizes in a monoclinic system with the $P2_1/c$ space group. The asymmetric unit incorporates one Cd^{2+} ion, two ntc$^-$ anions, one bmib ligand and one lattice water molecule (Fig. S5†). Similar with the cases of **1**−**4**, Cd^{2+} ion also is six-coordinated and has a distorted octahedral geometry, formed by four carboxylate oxygen atoms from two ntc$^-$ anions and two nitrogen atoms from a pair of bmib ligands. In this structure, bmib ligand is oriented in *anti-anti-anti* conformation, bridging the adjacent Cd^{2+} centers through the terminal N1 and N4 atoms along *b* axis, giving rise to an infinite zigzag chain with Cd···Cd of 14.1978(5) Å (Fig. 5a). The Cd^{2+} ions in these chains are bridged by μ-(η^1,η^1) carboxylate groups of ntc$^-$ anions, to balance the charges and consolidate the whole structure. Because of *in situ* decarboxylation of H$_2$ntdc plus the chelating fashion of ntc$^-$ anions, **5** finally does not propagate into a higher dimensional structure. However, the adjacent 1D chains are interlinked by intermolecular hydrogen bonding interactions between free water molecule and carboxylate oxygen atoms [O···O distances: O(9)···O(4) =2.923 Å, O(9)···O(6) =3.233 Å; and O–H···O angels: O(9)–H(1W)···O(4) =156.32°; O(9)–H(2W)···O(6) =179.43°], constructing a 2D hydrogen-bonded (4,4) **sql** layer (Fig. 5b and Fig. 5c). Moreover, the 2D layers are bound together to form a 3D supramolecular structure by π–π interactions varying from 3.6172(16) to 3.7809(16) Å.

Discussion structural diversity of CPs 1−4

The presence of the nitro group in H$_2$ntdc ligand, the flexibility of bis(imidazole) ligands with different substituents and spacers can greatly influence the assembly of the resulting architectures. Generally, the nitro group is not involved in coordination with transition metal ions, but its electronic nature and steric congestion can affect the coordination modes and the

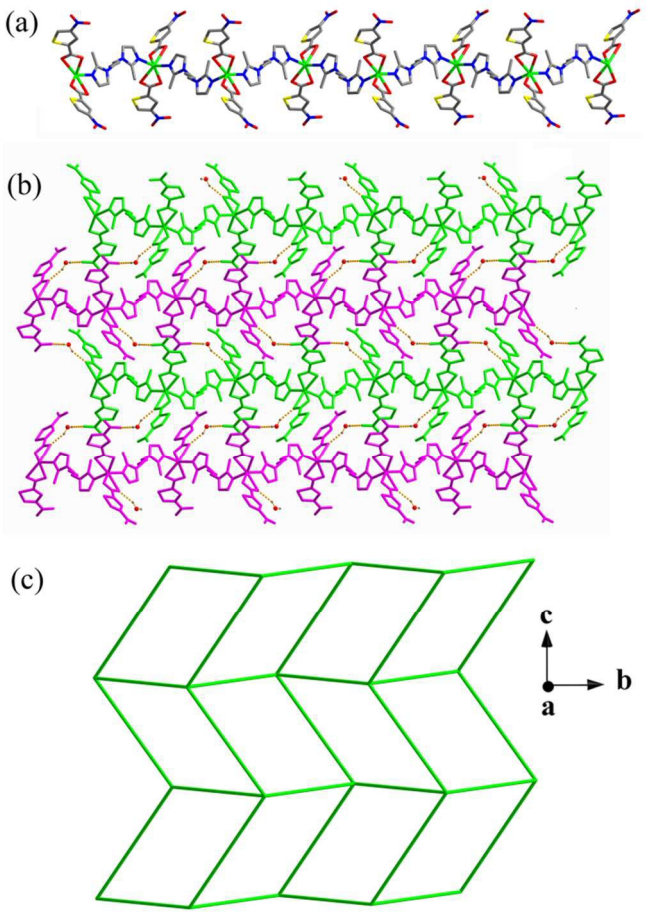

Fig. 5 (a) View of the polymeric zigzag chain in **5**. (b) View of the 3D supramolecular framework reinforced *via* O–H···O hydrogen bonding interactions. (c) Simplified view of the 2D hydrogen-bonded (4,4) **sql** layer of **5**. The hydrogen atoms are omitted for clarity.

coordinating ability of carboxylates when coordinated to metal ions.

As discussed above, H_2ntdc ligand presents three different coordination modes (Scheme 2). In **1**, each ntdc^{2-} anion in a bidentate μ_2-(η^1,η^1)-(η^1) bridging mode link Cd^{2+} ions, resulting in a 1D chain. In **2** and **3**, ntdc^{2-} anions take the same μ_3-(η^1,η^1)-(η^1,η^1) coordination mode to bridge Cd^{2+} ions. However, they yield different structures including 3-connected 2D **hcb** layer and a double chain structure due to different linking orientations of carboxylate groups. In **4**, each ntdc^{2-} anion serves as a bridge linking two adjacent Cd^{2+} ions by adopting μ_2-(η^1,η^1)-(η^1,η^1) coordination mode to generate a 1D zigzag chain. Therefore, it is reasonable that H_2ntdc is a versatile dicarboxylate ligand, and it can take adaptable coordination mode to generate diverse coordination architectures. What is more, C1–C2 bond distances observed in **1**–**4** are significantly (1.513 Å for **1**, 1.581 Å for **2** and 1.514 Å for **3**) or slightly (1.495 Å for **4**) longer than that found in CPs constructed from H_2tdc, which is also attributed to adjacent nitro group with the greater electron-withdrawing ability.

The methyl or ethyl on the imidazole ring can enhance the electron donating ability and steric hindrance to modulate the

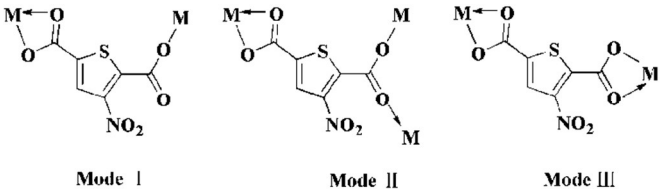

Scheme 2 Coordination modes of H_2ntdc ligand involved in **1**–**4**.

topologies. When bmip, bmib, beip and beib linkers are introduced into the assembled systems, the resulting CPs exhibit the 4^4-**sql** layer for **1**, 3,4-connected **ins** net for **2**, 3,5-connected net with $(4^2.6^3.8^5)(4^2.6)$ topology for **3** and 3-fold interpenetrating net with **dmp** topology for **4**, respectively. Furthermore, the bulky ethyl groups in beip and beib spacers are completely threaded into the lateral void of the adjacent layers, resulting in the absence of guest water molecules in **3** and **4**.

Discussion the structure of 5 involving *in situ* decarboxylation of H_2ntdc

On consideration of the structure, we think that **5** can not be obtained by single-crystal to single-crystal transformation of **2**, but generated from co-assembly of Hntc *in situ* generated, metal ions and bmib ligand. First, Hntc was easily obtained by heating the as-synthesized H_2ntdc at 120 °C in water. In the ^{1}H NMR spectrum of H_2ntdc, the peak at 4.79 ppm is attributed to H_2O, while the peak appears at 7.85 ppm that can be attributed to hydrogen atoms of the thiophene ring (Fig. S6†). Note that the –COOH hydrogen atoms are not observed, likely due to rapid H/D exchange. For Hntc, Peaks appear at 8.63 and 8.07 ppm can be assigned to thiophene hydrogen atoms. Secondly, as expected, **5** can be directly synthesized using the Hntc as a starting material. Thirdly, after crystals of **2** were obtained, this mixture was directly treated under the same condition as the synthesis of **5**. Powder X-ray diffraction (PXRD) pattern exhibits the resulting crystals remain **2**, which demonstrated that interconversion from **2** to **5** was not occurred. These observations clearly demonstrate thermal decarboxylation of H_2ntdc is prior to the formation of **5** under our experimental conditions, although there have been reports of decarboxylation reactions mediated by Cd^{2+} ions under hydro(solvo)-thermal conditions.[10] Notably, synthesis of thiophene derivatives has been a focus of research efforts because the thiophene nucleus is found in countless biologically active molecules and medicinally relevant structures. The transformation of Hntc using a simple *in situ* thermal decarboxylation of H_2ntdc in aqueous solution is straightforward and applicable. Moreover, on-going efforts are underway to investigate solid-phase organic chemistry studies of interconversion from H_2ntdc to Hntc.

PXRD, thermal stabilities and luminescence properties

Measured powder X-ray diffraction (PXRD) patterns of complexes **1**–**5** match very well with the simulated ones generated from the single crystal data (Fig. S7†). The main

difference in reflection intensities between the simulated and measured patterns was owing to the variation in the preferred orientation of the powder sample during the data collection. Thermogravimetric (TGA) experiments were carried out to study the thermal stabilities of **1**–**5** (Fig. S8†). In the TG curve of **1**, coordinated and lattice water molecules were lost from 75 to 180 °C (calcd.: 6.34%, found: 6.40%). Above 180 °C, the sample suffered an abrupt weight loss, indicating the collapse of the network. For **2**, the lattice water molecules were released from 40 to 60 °C (calcd.: 3.19%, found: 3.15%). The remaining substance is stable upon heating to 155 °C, and then the gradual and rapid weight decrease happened. For **3,** it can be stable under 230 °C and decomposed at higher temperature. Complex **4** is stable under 220 °C, and then it decomposed upon further heating. The lattice water molecules of **5** were released from 60 to 80 °C (calcd.: 2.60%, found: 2.58%). The network is thermally stable upon heating to 240 °C and then the continuous weight loss occurred.

Due to insoluble in common solvents, photoluminescence properties of CPs **1**−**4** in the solid state were measured at room temperature (Fig. S9†). Monitored at 300 nm excitation wavelength, the pure H_2ntdc displays a main emission centred at 474 nm, and the emission may be attributed to the $\pi^*\rightarrow\pi$ or $\pi^*\rightarrow n$ transition within the ligand. Upon excitation at 330 nm, main emissions bands are observed at 482 nm for **1**, 471 nm for **2**, 469 nm for **3** and 400 nm for **4**. Moreover, the bis(imidazole) ligands display luminescence emission bands at 410 nm (λ_{ex}= 300 nm) for bmip, 465 nm (λ_{ex}= 280nm) for bmib, 532 nm (λ_{ex}= 300 nm) for beip, and 403nm (λ_{ex}= 300 nm) for beib, respectively. It is well known that the Cd^{2+} ions are electrochemically inert due to the d^{10} configuration. When coordinated, Cd^{2+} ions can not accept electrons from ligands with their d-orbitals, nor donate electrons to ligands. Therefore, the shifts of these emission occurring in CPs **1**–**4** are probably due to the cooperative effects of intra-ligand emission, which are neither metal-to-ligand charge transfer (MLCT) nor ligand-to-metal charge transfer (LMCT) in nature.[11]

Conclusion

In this work, we have synthesized a new H_2ntdc ligand and demonstrated its utility in the formation of five cadmium CPs in the presence of four structurally related bis(imidazole) ligands. Structural diversities demonstrate that H_2ntdc can act as an excellent candidate to construct CPs. A straight forward synthesis of Hntc based on *in situ* decarboxylation of H_2ntdc in solution has also been carried out. Moreover, structure stabilities and photoluminescent properties were also investigated. This work will further enrich the synthesis and design of CPs constructed from thiophene-2,5-dicarboxylic acid derivatives, and the extendable work will construct CPs through employing analogous ligands *via* H_2tdc functionalization.

Acknowledgements

This work was supported by the National Natural Science Foundation of China (21401097 and 21371089), and sponsored by Program for New Century Excellent Talents in University (NCET-11-0947), Innovation Scientists and Technicians Troop Construction Projects of Henan Province (134100510011) and supported by Program for Innovative Research Team (in Science and Technology) in University of Henan Province.

Notes and references

[a]*College of Chemistry and Chemical Engineering, Luoyang Normal University, Luoyang, Henan 471022, P. R. China*
[b]*College of Chemistry and Pharmaceutical Engineering, Nanyang Normal University, Nanyang 473061, P. R. China.*
E-mail: mazhuxp@126.com, wlya@lynu.edu.cn

†Electronic Supplementary Information (ESI) available: crystal data for **1–5**, selected bond lengths, hydrogen bond parameters, PXRD, TG analysis, as well as luminescence properties and ^{1}H NMR spectroscopy. CCDC: 1047168-1047169 for complexes **1**−**2**, 1405270-1405271 for complexes **3**−**4** and 1047170 for complex **5**. For ESI and crystallographic data in CIF or other electronic format, See DOI:

1 (*a*) M. Eddaoudi, D. B. Moler, H. L. Li, B. L. Chen, T. M. Reineke, M. O'Keeffe and O. M. Yaghi, *Acc. Chem. Res*., 2001, **34**, 319; (*b*) D. Bradshaw, J. B. Claridge, E. J. Cussen, T. J. Prior and M. J. Rosseinsky, *Acc. Chem. Res*., 2005, **38**, 273; (*c*) S. Qiu and G. Zhu, *Coord. Chem. Rev*., 2009, **253**, 2891; (*d*) D. Zhao, D. J. Timmons, D. Yuan and H.-C. Zhou, *Acc. Chem. Res*., 2011, **44**, 123; (*e*) J. Liu, P. K. Thallapally, B. P. McGrail, D. R. Brown and J. Liu, *Chem. Soc. Rev.*, 2012, **41**, 2308; (*f*) K. Sumida, D. L. Rogow, J. A. Mason, T. M. McDonald, E. D. Bloch, Z. R. Herm, T.-H. Bae and J. R. Long, *Chem. Rev.*, 2012, **112**, 724; (*g*) M. Yoon, R. Srirambalaji and K. Kim, *Chem. Rev.*, 2012, **112**, 1196.

2 (*a*) M. Chen, S.-S. Chen, T.-A. Okamura, Z. Su, M.-S. Chen,Y. Zhao, W.-Y. Sun and N. Ueyama, *Cryst. Growth Des*., 2011, **11**, 1901; (*b*) D. Sun, Y.-H. Li,H.-J. Hao, F.-J. Liu, Y.-M. Wen, R.-B. Huang and L.-S. Zheng, *Cryst. Growth Des*., 2011, **11**, 3323;(*c*) C.-P. Li and M. Du, *Chem. Commun*., 2011, **47**, 5958; (*d*) S.-M. Fang, Q. Zhang, M. Hu, E. C. Sanudo, M. Du and C.-S. Liu, *Inorg. Chem*., 2010, **49**, 9617; (*e*) S.-I. Noro, R. Kitaura, M. Kondo, S. Kitagawa, T. Ishii, H. Matsuzaka and M. J. Yamashita, *J. Am. Chem. Soc*., 2002, **124**, 2568; (*f*) D. Sun, Z.-H. Wei, C.-F. Yang, D.-F. Wang, N. Zhang, R.-B. Huang and L.-S. Zheng, *CrystEngComm*, 2011, **13**, 1591; (*g*) X.-Z. Song, S.-Y. Song, M. Zhu, Z.-M. Hao, X. Meng, S.-N. Zhao and H.-J. Zhang, *Dalton Trans*., 2013, **42**, 13231.

3 (*a*) S. A. Bourne, J. J. Lu, A. Mondal, B. Moulton and M. J. Zaworotko, *Angew. Chem., Int. Ed.,* 2001, **40**, 2111; (*b*) W.-W. Dong, D.-S. Li, J. Zhao, Y.-P. Duan, L. Bai and J.-J. Yang, *RSC Adv*., 2012, **2**, 11219; (*c*) M. Chen, S.-S. Chen, Taka-aki Okamura, Z. Su, M.-S. Chen, Y. Zhao, W.-Y. Sun and N. Ueyama, *Cryst. Growth Des*., 2011, **11**, 1901; (*d*) B. Zhao, L. Yi, Y. Dai, X.-Y. Chen, P. Cheng, D.-Z. Liao, S.-P. Yan and Z.-H. Jiang, *Inorg. Chem*., 2005, **44**, 911; (*e*) Y.-T. Liu, Y.-Q. Du, X. Wu, Z.-P. Zheng, X.-M. Lin, L.-C. Zhu and Y.-P. Cai, *CrystEngComm*, 2014, **16**, 6797; (*f*) Y.-Q. Sun, J. Zhang, Y.-M. Chen and G.-Y. Yang, *Angew. Chem., Int. Ed*., 2005, **44**, 5814; (*g*) J. Zhang, J. T. Bu, S. Chen, T. Wu, S. Zheng, Y. Chen, R. A. Nieto, P. Feng and X. Bu, *Angew. Chem. Int. Ed*., 2010, **49**, 8876; (*h*) L.-P. Xue, X.-H. Chang, S.-H. Li, L.-F. Ma and L.-Y. Wang, *Dalton Trans*., 2014, **43**, 7219; (*i*) Z.-H. Li, T. Zhang, L-P. Xue, S.-B. Miao, B.-T. Zhao, J. Kan and W.-P. Su, *CrystEngComm*, 2013, **15**, 7423.

4 (*a*) L.-F. Ma, Q.-L. Meng, C.-P. Li, B. Li, L.-Y. Wang, M. Du and F.-P. Liang, *Cryst. Growth Des*., 2010, **10**, 3036; (*b*) L.-F. Ma, X.-Q. Li, Q.-L.Meng, L.-Y. Wang, M. Du and H.-W. Hou, *Cryst. Growth Des*., 2011, **11**, 175; (*c*) S. Sengupta, S. Ganguly, A. Goswami, P. K. Sukul and R. Mondal, *CrystEngComm*, 2013, **15**, 8353; (*d*) C.

Tian, Z. Lin and S. Du, *Cryst. Growth Des*., 2013, **13**, 3746; (*e*) A. Schoedel, W. Boyette, L. Wojtas, M. Eddaoudi and M. J. Zaworotko, *J. Am. Chem. Soc*., 2013, **135**, 14016; (*f*) D. -S. Zhou, F.-K. Wang, S.-Y. Yang, Z.-X. Xie and R.-B. Huang, *CrystEngComm*, 2009, **11**, 2548; (*g*) J. Chen, C. -P. Li and M. Du, *CrystEngComm*, 2011, **13**, 1885; (*h*) Y.-B. Zhang, H. Furukawa, N. Ko, W. Nie, H. Jeong Park, S. Okajima, K. E. Cordova, H. Deng, J. Kim and O. M. Yaghi, *J. Am. Chem. Soc*., 2015, **137**, 2641; (*i*) X. Li, Z. Yu, T. Guan, X. Li, G. Ma and X. Guo, *Cryst. Growth Des*., 2015, **15**, 278.

5 (*a*) S. K. Ghosh, J. Ribas, M. S. El Fallah and P. K. Bharadwaj, *Inorg. Chem*., 2005, **44**, 3856; (*b*) X.-L. Li, G.-Z. Liu, L.-Y. Xin and L.-Y. Wang, *CrystEngComm*, 2012, **14**, 880; (*c*) J.-H. Deng, D.-C. Zhong, X.-Z. Luo, H.-J. Liu and T.-B. Lu, *Cryst. Growth Des*., 2012, **12**, 4861; (*d*) X. Feng, J. Wang, B. Liu, L. Wang, J. Zhao and S. Ng, *Cryst. Growth Des*., 2012, **12**, 927; (*e*) C.-L. Guo, X. Zhuo, Y.-Z. Li and H.-G. Zheng, *Inorg. Chim. Acta,* 2009, **362**, 491.

6 (*a*) Y.-P. He, Y.-X. Tan and J. Zhang, *Cryst. Growth Des*., 2014, **14**, 3493; (*b*) Y. Takashima, C. Bonneau, S. Furukawa, M. Kondo, R. Matsuda and S. Kitagawa, *Chem. Commun*., 2010, **46**, 4142; (*c*) L. Zhou, C. Wang, X. Zheng, Z. Tian, L. Wen, H. Qu and D. Li, *Dalton Trans*., 2013, **42**, 16375; (*d*) L.-P. Xue, X.-H. Chang, L.-F. Ma and L.-Y. Wang, *RSC Adv*., 2014, **4**, 60883.

7 (*a*) H. Erer, O. Z. Yeşilel and M. Arıcı,*Cryst. Growth Des*., 2015, **15**, 3201; (*b*) H.-J. Hao, F.-J. Liu, H.-F. Su, Z.-H. Wang, D.-F. Wang, R.-B. Huang and L.-S. Zheng, *CrystEngComm*, 2012, **14**, 6726; (*c*) D. Sun, S. Yuan, H. Wang, H.-F. Lu, S.-Y. Feng and D.-F. Sun, *Chem. Commun***.**, 2013, **49**, 6152; (*d*) Y.-Y. Liu, C.-J. Wang and Y.-S. Yan, *Acta Cryst*., 2011, **E67**, m1544.

8 G. M. Sheldrick, *SADABS*, *Program for Siemens Area Detector Absorption Corrections*, University of Göttingen, Germany, 1997.

9 (*a*) G. M. Sheldrick, *SHELXTL Version 5.1. Bruker Analytical X-ray Instruments Inc*., Madison, Wisconsin, USA, 1998; (*b*) G. M. Sheldrick, SHELXL-97, *Program for the Refinement of Crystal Structure*; University of Göttingen, Germany, 1997.

10 (*a*)T.-W. Tseng, T.-T. Luo, S.-Y. Chen, C.-C. Su, K.-M. Chi and K.-L. Lu, *Cryst. Growth Des*., 2013, **13**, 510; (*b*) C. M. Gandolfo and R. L. LaDuca, *Inorg. Chem. Comm*., 2011, **14**, 1111.

11 (*a*) F.-F. Li, J.-F. Ma, S.-Y. Song, J. Yang, Y.-Y. Liu and Z.-M. Su, *Inorg. Chem*., 2005, **44**, 9374; (*b*) G. K. Walkup, S. C. Burdette, S. J. Lippard and R. Y. Tsien, *J. Am. Chem. Soc*., 2000, **122**, 5644; (*c*) X. L. Wang, C. Qin, E. B. Wang and Z. M. Su, *Chem.–A. Eur. J*., 2006, **12**, 2680.

Graphical Abstract:

Title: **Crystal engineering of cadmium coordination polymers decorated by nitro-functionalized thiophene-2,5-dicarboxylate and structurally related bis(imidazole) ligands with varying flexibility**

Key Topic:

Five bis(imidazole) ligands modulated Cadmium coordination polymers based on a new nitro-functionalized thiophene-2,5-dicarboxylate ligand or 4-nitro-thiophene-2-carboxylic acid involving *in situ* ligand synthesis.